Controlled shock loading conditions for micrstructural correlation of dynamic damage behavior

Darcie Dennis-Koller, J. Pablo Escobedo-Diaz, Ellen Cerreta, Curt A. Bronkhorst, Benjamin Hansen et al.

Citation: AIP Conf. Proc. **1426**, 1325 (2012); doi: 10.1063/1.3686525
View online: http://dx.doi.org/10.1063/1.3686525
View Table of Contents: http://proceedings.aip.org/dbt/dbt.jsp?KEY=APCPCS&Volume=1426&Issue=1
Published by the American Institute of Physics.

CONTROLLED SHOCK LOADING CONDITIONS FOR MICRSTRUCTURAL CORRELATION OF DYNAMIC DAMAGE BEHAVIOR

D. Dennis-Koller, J. P. Escobedo-Diaz, E. K. Cerreta, C. A. Bronkhorst, B. Hansen, R. Lebensohn, H. Mourad, B. Patterson, and D. Tonks

Los Alamos National Laboratory, Los Alamos NM 87545

Abstract. Materials performance is recognized as being central to many emergent technologies. Future technologies will place increasing demands on materials performance with respect to extremes in stress, strain, temperature, and pressure. In this study, the dynamic ductile damage evolution of OFHC Cu is explored as a test bed to understand the role of spatial effects due to loading profile and defect density. Well-characterized OFHC Cu samples of 30 μm, 60 μm, 100 μm, and 200 μm grain sizes were subjected to plate impact uniaxial strain loading at 1.5 GPa. This spall geometry produced early stage (incipient) damage in the Cu samples that could be correlated to microstructural features in metallographic analysis. The recovered damaged microstructure was examined using traditional 2D metallographic techniques (optical and electron microscopy) as well as 3D x-ray microtomography. Calculated spall strength from the free surface velocimetry (VISAR) showed no change with respect to changes in grain size, however, the magnitude of the peak after the first pull-back as well as rate of re-acceleration are dependent on grain size and can be correlated to damage observed in the recovered samples. These results reveal a critical length scale for the transition from a nucleation dominated regime to a growth dominated regime for the damage evolution process. The results show that for samples with small (30 μm) and large (200 μm) grain sizes the growth of voids is dominated by coalescence, whereas for medium (60 μm and 100 μm) grain sizes the growth is restricted to a much slower process of individual void growth. Electron backscatter diffraction reveals that voids preferentially nucleate at grain boundaries with high misorientation angles while special boundaries (low angle ∑1 and high angle ∑3) proved to be resistant to void nucleation. Based on these findings, mechanisms for the void nucleation/growth and coalescence are proposed.

Keywords: spall, fracture, OFHC Cu, soft recovery, shock wave shape.
PACS: 62.20mm, 81.40Np, 62.20F-.

INTRODUCTION

Materials are recognized as being central to many emergent technologies. Future technologies will place increasing demands on materials performance with respect to extremes in stress, strain, temperature, and pressure. Hence, it is not surprising that material failure and property degradation is a critical problem. This type of damage and failure is often linked to defects within the material and determines service lifetime. Dynamic material damage develops through an evolution of microstructural changes from the atomic scale to the macroscale damage event and is affected significantly by defects such as grain boundaries and inclusions within structural metals that typically serve as failure initiation sites. While

Shock Compression of Condensed Matter - 2011
AIP Conf. Proc. 1426, 1325-1330 (2012); doi: 10.1063/1.3686525
2012 American Institute of Physics 978-0-7354-1006-0/$0.00

for some defect types, their mere presence is enough to cause failure, for others, spatial considerations such as distribution or density can be critical [1]. Shock compression via plate impact is used to investigate dynamic damage processes because of the ability to control global one-dimensional, planar strain loading conditions and to recover the sample for metallurgical analysis. In a plate impact experiment, dynamic tensile damage occurs when rarefaction (decompression) waves within the target material interact to produce tensile stresses in excess of the yielding threshold required for damage initiation.

Extensive work to date has established that spall is a complex process strongly influenced by the dynamic loading profile or shock wave shape imparted to the specimen and microstructure [2-5]. However, while this is now generally accepted, the evolution of the tensile stress leading to yielding in the material is not well understood. Most of the cited work has focused on the effects on particle velocity pull-back measurements in experiments in which the sample experienced complete failure. This precludes any significant conclusion about the individual contributions of material characteristics from these measurements. The evolution of the tensile stress leading to damage is controlled by shock rise time, pulse duration, peak shock stress (compressive and tensile) and release rate. In addition, as the shock wave shape is altered experimentally, one important parameter that is frequently unaddressed is the coupling of that changing shock wave shape to the changes in the volume of material that is subjected to tension during a dynamic experiment. Figure 1 illustrates the effect of changes in shock wave shape (resulting from changes in impactor and target geometry) on the characteristics of the region of tension developed in the material leading to damage. Changes in pulse shape that significantly affect the volume of material being sampled in tension are believed to couple with microstructural length scales in a specimen to yield changes in the damage observed in soft recovered flyer plate experiments.

Incipient spall experiments are performed on high-purity copper samples with a known grain boundary density/distribution (grain size) to examine the relationship between these defect characteristics and void growth. Soft recovery of

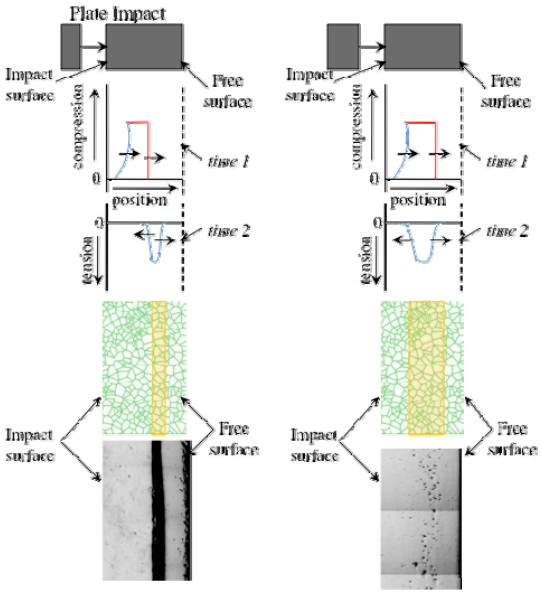

Figure 1 Time evolution of the stress profile in a material during a plate impact experiment in spall geometry. The effect of changing the experimental geometry results in a tensile region of different size forming in the material. Microstructural considerations include number of defect sites subjected to the tension evolved in the volume defined by a given geometry.

samples provides characterization of the end state, quantification of microstructural state and insipient damage.

EXPERIMENTAL PROCEDURE

Initial material characterization

All target materials were prepared from fully annealed 99.999% pure oxygen-free high-conductivity (OFHC) copper and have the same pedigree as the samples used in one of our earlier studies [6], in which the quasi-static compressive yield strength of copper revealed a very weak grain size dependency (< 5 MPa). The samples have average grain sizes of 30, 60, 100 and 200 μm following annealing under vacuum at 450° C for 30 min., 600° C for 1 hour, 850° C for 1 hour and 900° C for 35 min, respectively. It should be noted that not only was the defect density/distribution (grain boundary) strictly controlled, but the defect nature (grain boundary type) was, as well. In all cases, the textures and misorientation distributions are consistent with those typically obtained in recrystallized copper.

TABLE 1. Experimental data on microstructural length scale in OFHC Cu.

Experiment	Grain size, μm	Impactor thickness, mm	U_D, km/s	Target thickness, mm	Spall Strength, GPa
1s-1430	30	2.027	0.134	3.998	1.38
1s-1440	60	2.027	0.133	4.030	1.36
1s-1476	100	2.056	0.138	4.034	1.31
1s-1434	200	2.025	0.131	3.899	1.38

Subsequent characterization of the damage in the recovered samples included optical and EBSD microscopy. In preparation for the optical and EBSD analyses, each recovered specimen is diametrically sectioned. They are subsequently mounted in an epoxy resin and prepared following standard metallographic techniques up to a 0.05 μm colloidal silica final polish, performed on a vibratory polisher. Finally, they are electro-chemically polished using a solution of two parts of phosphoric acid to one part water at ~1.9 V for ~10 sec. A similar procedure is followed on the undeformed, as-annealed samples. Optical micros-copy was performed on a Zeiss microscope equipped with an automated stage. Image processing is done using Image J. EBSD is performed on a Phillips XL30 FEG SEM using a voltage of 20 kV and a spot size of 4.

Plate impact experiments

Plate impact experiments have been conducted using a smooth bore 78 mm light gas gun. A single well characterized loading condition is chosen for all experiments to ensure the kinetic aspects of the tensile stress profile evolution remain consistent for all experiments. The microstructural length scale is altered by changing the number of grain boundaries subjected to the tensile volume evolved by a given shock wave profile (controls defect density per unit volume). This is accomplished by using different grain sizes and identical shock loading profile (identical experimental geometry). Quartz impactors (z-cut, 2 mm nominal thickness) are mounted on Lexan sabots and launched using Ar gas. Quartz impactors ensure that a single, elastic shock wave is produced in the stress range of interest to this study. Table 1 lists the experimental details (stress calculations are discussed in the next section).

To ensure that the recovered samples are subjected to only a known uniaxial loading and unloading history, significant radial release is minimized through the use of momentum trapping rings (technique described elsewhere [6])

After assembly, the parallelism, of the sample to the target plate, and the height of each pin with respect to the target plate is measured. Velocimetry profiles are obtained using a VISAR [7] system (spot size ~0.5 to 1 mm diameter) mounted 90° off of the shock direction axis to prevent the target from impacting the probe. In all cases shots are performed between two and four times to test repeatability as well as generate statistically accurate measurements of damage distributions

RESULTS AND DISCUSSION

Figure 2 shows the free surface velocity (FSV) histories for the microstructural length scale experiments. Experimental parameters are listed in Table I along with calculated spall strength. The peak free surface velocities range from 82 to 84 m/s, corresponding to peak compressive stresses of 1.50 – 1.56 GPa. These values are calculated using the Mie Grüneisen equation of state for copper: ρ_o = 8.924 g/cm^3 (density), C_o = 3.94 mm/μs (bulk sound speed), s = 1.489 and γ = 1.96. The spall strength (σ_{spall}) is calculated using the relationship for a material that exhibits an elasto-plastic behavior [8]:

$$\sigma_{spall} \equiv \rho_0 C_L \Delta FSV \left(1 + \frac{C_L}{C_o}\right)^{-1} \qquad \text{Eq. (1)}$$

where C_L = 4.77 mm/μs is the longitudinal sound speed and ΔFSV is the difference in free surface velocity from the peak state to the minima after release. The measured and calculated experimental parameters are listed in Table 1. It is found that by holding the loading profile constant (i.e peak stress and experimental geometry identical for each experiment), the calculated spall strength is ~ 1.31 to 1.38 GPa with no clear influence of the grain size.

TABLE 2. Experimental data on microstructural length scale in OFHC Cu.

Experiment	Grain size, μm	Void count	Void area fraction, %	Avg. void diameter, μm	$V_{sp\text{-}pk}/V_{comp}$
1s-1430	30	236	0.496	38.1	0.214
1s-1440	60	343	0.249	22.7	0.349
1s-1476	100	267	0.416	33.0	0.345
1s-1434	200	111	0.507	55.1	0.231

However, differences are observed in the pull back response after the release. The magnitude of the first pull back and the rate at which the velocity rises to the first peak (i.e. spall peak) after the release are indicative of the mechanisms involved in the yielding process. Figure 3 shows the pull back signals for each experiment (from the minima reached after release to the spall peak velocity reached in the pull back). The times and velocities are shifted so that the minima coincides with the origin in the plot.

In a qualitative manner, Cochran and Banner [9] showed that the ratio of the spall peak particle velocity ($V_{sp\text{-}pk}$) with respect to the peak particle velocity on compression (V_{comp}) is indicative of the observed void density in the recovered sample.

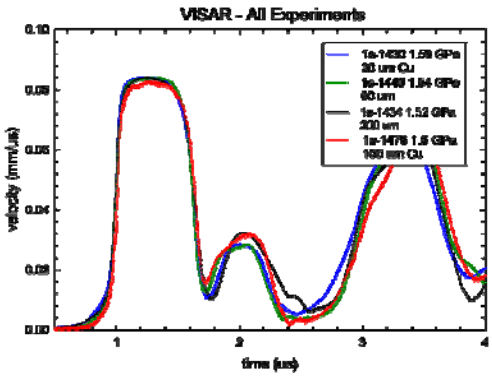

Figure 2 VISAR results for the free surface velocity of OFHC Cu of 4 different grain sizes. While all shock wave shapes agree through the release, the response after the pullback shows differences in the yielding response and can be correlated to microstructural features in the recovered samples.

Essentially, they observed that as the pull back signal increases in magnitude (as the difference between V_{comp} and $V_{sp\text{-}pk}$ gets smaller) the amount of observed damage in also increased. Table II lists the ratio of these velocities for the current experiments. Figure 4 shows observed void area fraction from the recovered samples in these experiments plotted against grain size and it follows a trend similar to that expected by Cochran and Banner. The larger the difference between V_{comp} and $V_{sp\text{-}pk}$; the larger the void area fraction observed in the recovered sample.

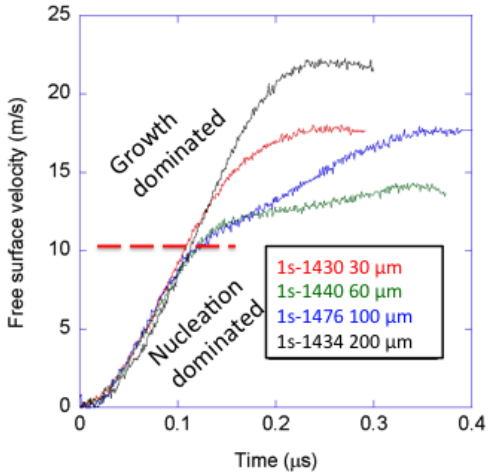

Figure 3. VISAR pull back where all minima after the release have been normalized to zero. In all experiments the initial particle acceleration is similar. A mechanism change from nucleation dominated processes to growth dominated processes leads to a regime where micro-structural length scale (grain size) controls growth mechanism (coalescence dominated results in high particle acceleration and individual void growth results in lower particle acceleration).

In ductile materials, the rate at which the velocity pull back rises to the spall peak is qualitatively related to the void growth rate. The acceleration in the free surface velocity can be correlated with the velocity gradient of the wave reflected off the spall plane [8]. The velocity of this wave varies from C_L, in cases where there is a rapid fracture process; to C_0 in the cases where there is a stress relaxation due to a resistance in void growth which leads to lower damage rates [10]. Thus, shorter rise times to the spall peak correlate with a more rapid completion of the damage. In these experiments, the 30 and 200 µm samples exhibit a monotonic rise from the minima to the spall peak, indicative of a fast damage evolution process. Conversely, 60 and 100 µm samples experience a fast rise time initially, which subsequently displays a distinctive change in slope. This is indicates the dominate damage evolution mechanism undergoes a change. Figure 5 shows the optical micrographs of cross sections taken from the recovered samples. Figure 6 shows EBSD from those same cross sections.

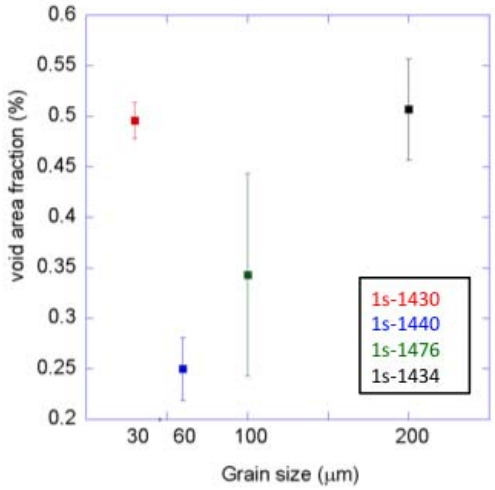

Figure 4. Void area fraction measured from recovered samples indicates that identical loading for the cases of large grain size and small grain size the void field is larger or more developed, whereas for mid size grains the void field is smaller or less developed.

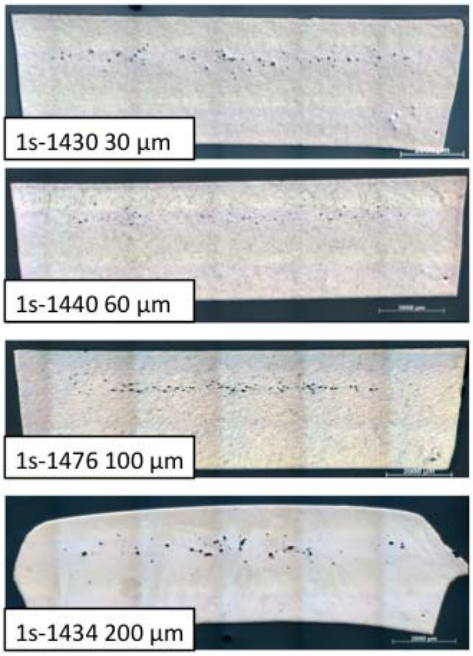

Figure 5. Optical micrographs of the cross sections taken from the recovered Cu samples shows qualitatively the observed difference in damage field due only to differences in grain size under identical loading conditions.

CONCLUSIONS

In these experiments the samples are subjected to identical loading conditions (geometry, peak pressure, etc.). Drawing conclusions from continuum level measurements such as free surface velocity and correlating them to the mesoscale microstructural processes is accomplished through careful model driven experimental design coupled with metallographic analysis of recovered test materials. In particular, it has been found that in spite of identical loading conditions the calculated spall strength remains comparable in all experiments with no dependence on grain size. The free surface velocity acceleration after the pull-back minima correlates with void growth mechanism, in which higher rates (observed in the 30 µm and 200 µm experiments) rendered larger voids indicative of a coalescence dominated growth mechanism rather than growth of individual voids. Interestingly, the samples that show a change in slope of the free surface velocity after the minima, present higher average kernel misorientations (60

μm and 100 μm experiments). This is indicative of the competition between void growth and plastic dissipation processes that is the result of individual void growth in the absence of significant coalescence. In all experiments, nucleation and growth are likely occurring simultaneously. However, early in time during the yielding process the dominate mechanism is nucleation of voids until a change in mechanism leads to a growth dominated regime. During the growth dominated regime, microstructural length scale dictates the type of growth mechanism (coalescence or individual void growth) that results in the rate of total damage evolution observed in the particle velocity.

ACKNOWLEDGEMENTS

This work was carried out under the auspices of U.S. DOE at LANL under contract DE-AC52-06NA25396. LDRD DR project 20100026DR.

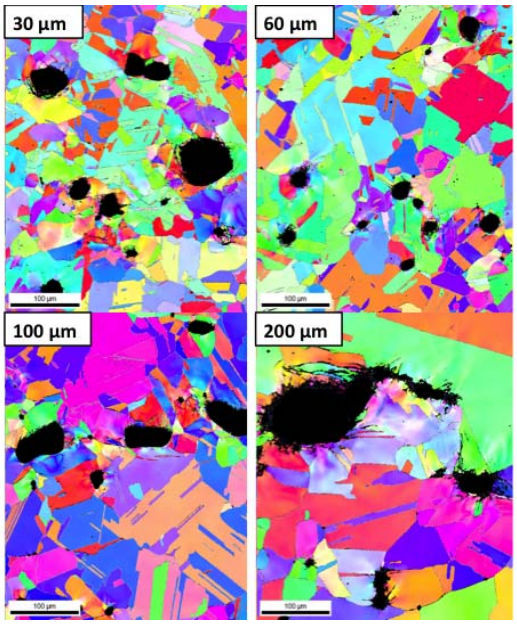

Figure 6 EBSD images of the cross sections of the Cu show that for small and large grain sizes larger coalesced voids are observed. In the cases of the mid grain sizes voids are largely isolated no significant coalescence is observed.

REFERENCES

1. Reid, C., Metal. Trans. A **12**, pp 371-377 (1981).
2. Kumar, M., AlChE Annual Meeting, Conf. Proc., 2541 (2005).
3. Curran, D. R., Seaman, L., and Shockey, D. A., Phys. Today **30**, 46 (1977).
4. Barbee, T. W., Seaman, L., Crewdson, R., and Curran, D. R., J. Mater. **7**, pp 393-401 (1972).
5. Johnson, J. N., Gray III, G. T., and Bourne, N. K., J. Appl. Phys. **86**, pp 4892-4901 (1999).
6. Koller, D. D., et al., J. Appl. Phys. **98**, pp 103518-1-7 (2005).
7. Hemsing, W. F., Rev. Sci. Instrum. **50**, pp 73-78 (1979).
8. Kanel, G. I., J. Appl. Mech. Tech. Phys. **42**, pp 358-362 (2001).
9. Cochran, S., and Banner, D., J. Appl. Phys. **48**, pp 2729-2737 (1977).
10. Kanel, G. I., Razorenov, S. V., Utkin, A. V., and Grady, D. E., AIP Conf. Proc. **370**, pp 503-506 (1996).